5126 *Inorg. Chem.* **1993,** *32,* 5126–5131

Synthesis and Characterization of Gold(I) Thiolates, Selenolates, and Tellurolates: X-ray Crystal Structures of $Au_4[TeC(SiMe_3)_3]_4$, $Au_4[SC(SiMe_3)_3]_4$, and $Ph_3PAu[TeC(SiMe_3)_3]$

Philip J. Bonasia, David E. Gindelberger, and John Arnold*

Department of Chemistry, University of California, Berkeley, California 94720

Received May 18, 1993●

We describe the preparation of a series of homoleptic gold(I) chalcogenolates of empirical formula Au[ER] (E = S, Se, Te; R = $C(SiMe_3)_3$, $Si(SiMe_3)_3$, $Ge(SiMe_3)_3$), by reaction of the appropriate lithium salts, LiER, with AuCl(THT) (THT = tetrahydrothiophene) in benzene or hexane. Metatheses between LiER and Ph_3PAuCl in diethyl ether afford the (triphenylphosphine)gold(I) complexes $Ph_3PAu[ER]$. The derivatives $Au_4[TeC(SiMe_3)_3]_4$ and $Ph_3PAu[TeC(SiMe_3)_3]$ are the first gold tellurolates reported, and both have been structurally characterized by X-ray crystallography. $Au_4[TeC(SiMe_3)_3]_4$ crystallizes at ambient temperatures from warm benzene in the space group $P2_12_12_1$ with $a = 15.295(2)$ Å, $b = 16.011(2)$ Å, $c = 29.971(6)$ Å, $V = 7340(4)$ Å^3, $d_{calcd} = 2.013$ g cm^{-3}, and $Z = 4$. $Ph_3PAu[TeC(SiMe_3)_3]$ crystallizes from ether at -40 °C in the space group $P2_1/n$ with $a = 9.748(3)$ Å, $b = 21.472(5)$ Å, $c = 15.684(3)$ Å, $\beta = 100.37(2)°$, $V = 3229(1)$ Å^3, $d_{calcd} = 1.683$ g cm^{-3}, and $Z = 4$. The thiolate analogue $Au_4[SC(SiMe_3)_3]_4$ has also been structurally characterized for comparison: this crystallizes from hexane at –40 °C in the space group $P2_1/c$ with $a = 14.976(2)$ Å, $b = 18.99(1)$ Å, $c = 27.622(5)$ Å, $\beta = 102.83(2)°$, $V = 7659(5)$ Å^3, $d_{calcd} = 1.598$ g cm^{-3}, and $Z = 4$; one molecule of disordered hexane is associated with each tetramer in the asymmetric unit.

Introduction

While the clinical use of compounds such as gold(I) thiomalate,[1,2] gold(I) thioglucose,[3] and (triethylphosphine)gold 2,3,4,6-tetra-*O*-acetyl-1-thio-*β*-D-glucopyranoside[3,4] for the treatment of rheumatoid arthritis[5,6] has unquestionably provided an impetus to study the chemistry of gold thiolates, related chemistry involving selenolates and tellurolates has scarcely been explored. In addition to further potential chemotherapeutic uses in the treatment of arthritis and cancer,[3,7] gold chalcogenolates have already begun to find applications in the sensitization of photographic materials,[8] electron microscopy,[5] and the preparation of conducting, semiconducting, and laser recording devices.[5]

Recently, a number of reports of (triphenylphosphine)gold(I) chalcogenolates, Ph_3PAuER (E = S, Se; R = alkyl, aryl), have appeared in the literature.[9–15] The only example of a homoleptic gold(I) chalcogenolate has been the hexameric gold(I) thiolate $[(2,4,6\text{-}^iPr_3C_6H_2S)Au]_6$, prepared by Strähle.[16] Although several gold(I) and gold(III) tellurides have been prepared and structurally characterized (*e.g.* $[Ph_4P]_4[KAu_9Te_7]^{-4}$,[17] $[Ph_4P]_2[K_2Au_4Te_4(en)_4]^{-2}$,[17] $[Ph_4P]_2[K_2Au_4Te_4(dmf)_2(CH_3OH)_2]^{-2}$,[17] and $(PPN)_2Au_2Te_4$[18]), to the best of our knowledge there have been no reports of gold tellurolates. Here we describe the chemistry of new homoleptic gold(I) chalcogenolates, Au[ER] (E = S, Se, Te; R = $C(SiMe_3)_3$, $Si(SiMe_3)_3$, $Ge(SiMe_3)_3$), prepared by metathesis of the appropriate lithium salt with AuCl(THT), and their adducts with triphenylphosphine.

Experimental Section

Our standard operating procedures were as described previously.[19,20] The starting materials AuCl(THT),[21] $(THF)_2LiTeC(SiMe_3)_3$,[22–24] $(THF)_2LiTeSi(SiMe_3)_3$,[19] $(THF)_2LiTeGe(SiMe_3)_3$,[22] $(DME)LiSeC(SiMe_3)_3$,[22,23] $(THF)_{1.5}LiSC(SiMe_3)_3$,[22,25] $(THF)LiSSi(SiMe_3)_3$,[22] $HSeC(SiMe_3)_3$,[22,26] $Ph_3PAuN(SiMe_3)_2$,[27] and $HSSi(SiMe_3)_3$[22,28] were all prepared as previously reported in the literature. Ph_3PAuCl was from Aldrich and was used as received.

$Au_4[TeC(SiMe_3)_3]_4$ (1). Via cannula, a solution of $(THF)_2LiTeC(SiMe_3)_3$ (0.67 g, 1.3 mmol) in benzene (40 mL) was added to AuCl(THT) (0.42 g, 1.3 mmol) suspended in benzene (25 mL). A black precipitate immediately formed, which on settling, revealed a dark yellow solution. The mixture was stirred for 18 h and then allowed to settle. Filtration of the brown-yellow solution and removal of the solvent under reduced pressure left a colorless solid (0.31 g, 42%). Slow crystallization at ambient temperature from warm benzene afforded X-ray-quality crystals of the tetrameric gold tellurolate. On heating in a melting point capillary, the colorless crystals decomposed slowly, forming a gold mirror by 220 °C and liberating the dialkyl telluride, $(Me_3Si)_3CTeC(SiMe_3)_3$, as a yellow condensate. (For $(Me_3Si)_3CTeC(SiMe_3)_3$, MS (EI, 70 eV): *m/z* 592 (M$^+$), 520 (M$^+$ – SiMe$_3$), 433, 361.) IR: 1268 sh, m, 1251 s, 842 s, 676 s, 649 s, 615 w, 588 m cm^{-1}. ^{1}H NMR (400 MHz, C_6D_6):

● Abstract published in *Advance ACS Abstracts*, October 1, 1993.

(1) Isab, A. A.; Sadler, P. J. *J. Chem. Soc., Dalton Trans.* **1981**, 1657.
(2) Isab, A. A.; Sadler, P. J. *J. Chem. Soc., Dalton Trans.* **1982**, 135.
(3) *Gold 100*; Gafner, G., King, R. P., Eds.; SAIMM Publications: Johannesburg, 1986; Vol. 3.
(4) Brown, D. H.; Smith, W. E. *Chem. Soc. Rev.* **1980**, *9*, 217.
(5) Raptis, R. G.; Murray, H. H., III; Fackler, J. P., Jr. *J. Chem. Soc., Chem. Commun.* **1987**, 737.
(6) Cotton, F. A.; Wilkinson, G. *Advanced Inorganic Chemistry*, 5th ed.; Wiley: New York, 1988.
(7) *Platinum, Gold and Other Metal Chemotherapeutic Agents: Chemistry and Biochemistry;* Lippard, S. J., Ed.; ACS Symposium Series, No. 209 American Chemical Society: Washington, DC, 1983.
(8) Marbach, G.; Strähle, J. *Angew. Chem., Int. Ed. Engl.* **1984**, *23*, 715.
(9) Jones, P. G.; Sheldrick, G. M.; Hädicke, E. *Acta Crystallogr.* **1980**, *B36*, 2777.
(10) Jones, P. G.; Thöne, C. *Chem. Ber.* **1990**, *123*, 1975.
(11) Wagner, I.; Du Mont, W.-W. *J. Organomet. Chem.* **1990**, *395*, C23.
(12) Wang, S.; Fackler, J. P., Jr. *Inorg. Chem.* **1990**, *29*, 4404.
(13) Jones, P. G.; Thöne, C. *Chem. Ber.* **1991**, *124*, 2725.
(14) Jones, P. G.; Thöne, C. *Inorg. Chim. Acta* **1991**, *181*, 291.
(15) Delgado, E.; Hernandez, E. *Polyhedron* **1992**, *11*, 3135.
(16) Schröter, I.; Strähle, J. *Chem. Ber.* **1991**, *124*, 2161.
(17) Haushalter, R. C. *Angew. Chem., Int. Ed. Engl.* **1985**, *24*, 432.
(18) Haushalter, R. C. *Inorg. Chim. Acta* **1985**, *102*, L37.
(19) Bonasia, P. J.; Gindelberger, D. E.; Dabbousi, B. O.; Arnold, J. *J. Am. Chem. Soc.* **1992**, *114*, 5209.
(20) Bonasia, P. J.; Arnold, J. *Inorg. Chem.* **1992**, *31*, 2508.
(21) Uson, R.; Laguna, A.; Laguna, M. *Inorg. Synth.* **1989**, *26*, 86.
(22) Bonasia, P. J.; Christou, V.; Arnold, J. *J. Am. Chem. Soc.* **1993**, *115*, 6777.
(23) Sladky, F.; Bildstein, B.; Rieker, C.; Gieren, A.; Betz, H.; Hubner, T. *J. Chem. Soc., Chem. Commun.* **1985**, 1800.
(24) Köllemann, C.; Obendorf, D.; Sladky, F. *Phosphorus Sulfur* **1988**, *38*, 69.
(25) Aslam, M.; Bartlett, R. A.; Block, E.; Olmstead, M. M.; Power, P. P.; Sigel, G. E. *J. Chem. Soc., Chem. Commun.* **1985**, 1674.
(26) Bildstein, B.; Giselbrecht, K.; Sladky, F. *Chem. Ber.* **1989**, *122*, 2279.
(27) Shiotani, A.; Schmidbaur, H. *J. Am. Chem. Soc.* **1970**, *92*, 7003.
(28) Ballestri, M.; Chatgilialoglu, C.; Seconi, G. *J. Organomet. Chem.* **1991**, *408*, C1.

0020-1669/93/1332-5126$04.00/0

δ 0.53 (s). $^{13}C\{^1H\}$ NMR (C_6D_6): δ 4.9. $^{125}Te\{^1H\}$ NMR (C_6D_6, 0.04 M): δ –302 ($\Delta\upsilon_{1/2}$ = 49 Hz). Anal. Calcd for $C_{40}H_{108}Au_4Si_{12}Te_4$: C, 21.6; H, 4.89. Found: C, 21.7; H, 4.80.

$Au_4[SeC(SiMe_3)_3]_4$ (2). (DME)$LiSeC(SiMe_3)_3$ (0.38 g, 0.94 mmol) dissolved in benzene (25 mL) was added to AuCl(THT) (0.30 g, 0.94 mmol) suspended in benzene (25 mL). The solution immediately became dark brown-yellow, and a black, flocculent precipitate formed. The solution was stirred for 2 h and allowed to settle. Filtration afforded a yellow solution, which was exposed to vacuum and dried to a pale yellow powder (0.31 g, 65%) that was pure by ^1H NMR measurements. Alternatively, recrystallization from hexane solutions at –40 °C led to large, colorless rectangular prisms that quickly became opaque on slight drying under vacuum. On heating, these crystals slowly became purple by 200 °C and finally decomposed between 230 and 240 °C, forming a gold mirror in the melting point capillary and releasing a clear condensate. IR: 1268 sh, m, 1254 s, 849 s, 774 m, 682 m, 651 m, 616 w, 598 w cm^{-1}. ^1H NMR (400 MHz, C_6D_6): δ 0.53 (s). $^{13}C\{^1H\}$ NMR (C_6D_6): δ 3.7. $^{77}Se\{^1H\}$ NMR (C_6D_6, 0.27 M): δ –124 ($\Delta\upsilon_{1/2}$ = 50 Hz). Anal. Calcd for $C_{40}H_{108}Au_4Si_{12}Se_4$: C, 23.7; H, 5.36; Found: C, 23.9; H, 5.39.

$Au_4[SC(SiMe_3)_3]_4$ (3). $(THF)_{1.5}LiSC(SiMe_3)_3$ (0.49 g, 1.3 mmol) was added to AuCl(THT) (0.42 g, 1.3 mmol) in benzene (25 mL). The cloudy suspension immediately became clear. The solution was stirred for 2 h and filtered, affording a pale yellow solution. This was dried under vacuum to give a yellow powder (0.42 g, 69%) that was pure by ^1H NMR measurements. Again, recrystallization from hexane at –40 °C led to colorless, cubic crystals. Correct elemental analyses were obtained when one-fourth of a molecule of hexane was factored into the material's empirical formula (see below). These crystals slowly became purple by 200 °C, finally decomposing by 280 °C; a clear condensate was again noted in the top of the melting point capillary. IR: 1268 sh, w, 1249 m, 850 s, 773 w, 679 w, 661 w, 614 w cm^{-1}. ^1H NMR (300 MHz, C_6D_6): δ 0.54 (s). $^{13}C\{^1H\}$ NMR (C_6D_6): δ 3.46. Anal. Calcd for $C_{40}H_{108}Au_4S_4Si_{12}\cdot{}^1/_4\,C_6H_{14}$: C, 28.7; H, 6.38; Found: C, 28.4; H, 6.30.

$Ph_3PAu[TeC(SiMe_3)_3]$ (4). Via cannula, $(THF)_2LiTeC(SiMe_3)_3$ (0.41 g, 0.81 mmol) dissolved in 40 mL of ether was added to a stirred suspension of PPh_3AuCl (0.40 g, 0.81 mmol) in diethyl ether (20 mL). The pale orange mixture reacted slowly and began to take on a red color after 15 min. After 24 h the brown-yellow solution was filtered into a Schlenk flask and the solvent was removed under vacuum, leaving a yellow powder. This was extracted with diethyl ether (25 mL), the extract was filtered, and the filtrate was concentrated to ca. 5 mL and cooled to –40 °C. After 24 h, filtration afforded 0.43 g (65%) of the product as yellow prisms. The crystals slowly decomposed above 130 °C, forming a gold mirror. IR: 1477 m, 1437 s, 1259 m, 1247 s, 1184 w, 1100 s, 1027 w, 995 w, 850 s, 765 w, 747 w, 740 s, 710 m, 695 s, 687 s, 650 s, 615 w, 582 m, 532 s, 505 s, 495 s cm^{-1}. ^1H NMR (400 MHz, C_6D_6): δ 7.40 (m, 6 H), 6.95 (m, 9 H), 0.60 (s, 27 H). $^{13}C\{^1H\}$ NMR (C_6D_6): δ 134.4, 134.2, 131.0, 129.2, 129.1, 5.24. $^{31}P\{^1H\}$ NMR (C_6D_6): δ 39.5 ($\Delta\upsilon_{1/2}$ = 235 Hz). $^{125}Te\{^1H\}$ NMR (C_6D_6, 0.12 M): δ –148 ($\Delta\upsilon_{1/2}$ = 41 Hz). Anal. Calcd for $C_{28}H_{42}AuPSi_3Te$: C, 41.1; H, 5.17. Found: C, 41.1; H, 5.00.

$Ph_3PAu[SeC(SiMe_3)_3]$ (5). Method A. (DME)$LiSeC(SiMe_3)_3$ (0.30 g, 0.74 mmol) dissolved in ether (40 mL) was added to a stirred suspension of Ph_3PAuCl (0.37 g, 0.74 mmol) in diethyl ether (20 mL). Over a period of several hours the stirred reaction mixture appeared to darken. After 12 h, the gray-blue solution was pumped to dryness under reduced pressure and re-extracted with ether (50 mL), and the extract was filtered. The yellow solution was concentrated to 10 mL and cooled to –40 °C overnight. Filtration afforded large, clear, colorless crystals (0.43 g, 75%) of the gold selenolate.

Method B. $HSeC(SiMe_3)_3$ (0.15 g, 0.48 mmol) dissolved in 30 mL of hexane was added to $Ph_3PAuN(SiMe_3)_2$ (0.30 g, 0.48 mmol) suspended in hexane (25 mL). As the selenol was added, the reaction mixture became cloudy yellow, and the white product began to precipitate from solution. After overnight stirring, the volatiles were removed under reduced pressure and the white solid was extracted with ether (40 mL). Concentration to ca. 10 mL and cooling to –40 °C for 12 h afforded the desired product as clear, colorless crystals (0.28 g, 76%). These appeared to decompose to a metallic material by 150 °C before melting to a black liquid from 184 to 189 °C. IR: 1475 s, 1434 s, 1328 m, 1244 s, 1178 s, 1097 s, 1068 w, 1024 m, 995 w, 852 s, 771 m, 746 s, 709 s, 691 s, 654 s, 614 m, 530 s, 500 s cm^{-1}. ^1H NMR (400 MHz, C_6D_6): δ 7.39 (m, 6 H), 6.95 (m, 9 H), 0.58 (s, 27 H). $^{13}C\{^1H\}$ NMR (C_6D_6): δ 134.4, 134.2, 131.3, 129.2, 129.1, 3.94. $^{31}P\{^1H\}$ NMR (C_6D_6): δ 37.61. MS (EI, 70 eV): *m/z* 769 (M^+), 622 $[(Me_3Si)_3CSe]_2$. Anal. Calcd for $C_{28}H_{42}AuPSi_3Se$: C, 43.7; H, 5.50. Found: C, 43.7; H, 5.55.

$Ph_3PAu[SC(SiMe_3)_3]$ (6). $(THF)_{1.5}LiSC(SiMe_3)_3$ (0.31 g, 0.81 mmol) dissolved in 25 mL of ether was added to Ph_3PAuCl (0.40 g, 0.81 mmol) suspended in 30 mL of diethyl ether, and the reaction mixture was left to stir overnight. The ether was removed under reduced pressure, and the pale yellow-white solid was extracted with ether (35 mL), the extract was filtered, and the filtrate was concentrated to 3 mL. Cooling of this solution to –40 °C for 48 h afforded the compound as large, clear, colorless, rectangular prisms that became opaque on drying (0.40 g, 69%). The crystals slowly became purple on heating and then melted quickly from 204 to 207 °C, forming a gold mirror. IR: 1479 sh, w, 1435 s, 1254 s, 1243 s, 1182 w, 1100 s, 1026 w, 997 w, 850 s, 777 m, 746 s, 711 m, 691 s, 674 sh, w, 614 w, 535 s, 504 s cm^{-1}. ^1H NMR (400 MHz, C_6D_6): δ 7.40 (m, 6 H), 6.93 (m, 9 H), 0.57 (s, 27 H). $^{13}C\{^1H\}$ NMR (C_6D_6): δ 134.4, 134.3, 131.29, 131.27, 130.5, 129.2, 129.1, 3.15. $^{31}P\{^1H\}$ NMR (C_6D_6): δ 38.4. Anal. Calcd for $C_{28}H_{42}AuPSSi_3$: C, 46.5; H, 5.86. Found: C, 45.9; H, 5.78.

Silane- and Germanetellurolates. *The silane- and germanetellurolates **7–10** are thermally unstable in solution. They must be prepared and handled at low temperature. A general experimental procedure for these compounds is given below, followed by their spectroscopic data.*

A solution of the lithium silane or germanetellurolate in ether at –78 °C was added to the appropriate gold reagent (AuCl(THT) or Ph_3PAuCl) in ether, also at –78 °C. The mixture was allowed to stir for 30 min, the reaction flask was removed from the cold bath, and the ether was quickly removed under reduced pressure. Attempts to purify the products resulted in decomposition. The products, though contaminated with LiCl, were sufficiently pure for use in subsequent reactions. In solution, they decomposed slowly over a period of approximately 24 h; as solids, they were thermally unstable but survived brief exposure to both air and water.

$Au[TeSi(SiMe_3)_3]$ (7). IR: 1268 sh, m, 1237 s, 838 s, 737 w, 685 m, 620 m, 509 w cm^{-1}. ^1H NMR (400 MHz, C_6D_6): δ 0.49. $^{13}C\{^1H\}$ NMR (C_6D_6): δ 1.79. $^{125}Te\{^1H\}$ NMR (C_6D_6, 20 °C, 0.07 M): δ –1112.

$Au[TeGe(SiMe_3)_3]$ (8). IR: 1268 sh, w, 1238 s, 832 s, 744 w, 685 m, 615 m cm^{-1}. ^1H NMR (400 MHz, C_6D_6): δ 0.53. $^{13}C\{^1H\}$ NMR (C_6D_6): δ 2.46. $^{125}Te\{^1H\}$ NMR (C_6D_6, 20 °C, 0.13 M): δ –1093.

$Ph_3PAu[TeSi(SiMe_3)_3]$ (9). IR: 1480 sh, m, 1435 s, 1255 sh, w, 1241 s, 1180 w, 1098 m, 1028 w, 995 w, 834 s, 745 m, 708 w, 691 s, 623 m, 530 s, 506 w, 495 w cm^{-1}. ^1H NMR (400 MHz, C_6D_6): δ 7.41 (m, 6 H), 6.96 (m, 9 H), 0.47 (s, 27 H). $^{13}C\{^1H\}$ NMR (C_6D_6): δ 134.4, 134.2, 131.0, 129.1, 129.0, 1.38. $^{31}P\{^1H\}$ NMR (C_7D_8, –70 °C): δ 42.5 ($\Delta\upsilon_{1/2}$ = 985 Hz).

$Ph_3PAu[TeGe(SiMe_3)_3]$ (10). IR: 1479 sh, w, 1435 s, 1255 sh, w, 1240 s, 1179 w, 1098 m, 1027 w, 996 w, 836 s, 743 m, 708 w, 691 s, 618 m, 528 s, 508 m, 495 m cm^{-1}. ^1H NMR (400 MHz, C_6D_6): δ 7.42 (m, 6 H), 6.97 (m, 9 H), 0.49 (s, 27 H). $^{13}C\{^1H\}$ NMR (C_6D_6): δ 134.3, 134.2, 130.3, 129.0, 128.9, 1.95. $^{31}P\{^1H\}$ NMR (C_7D_8, –70 °C): δ 44.1 ($\Delta\upsilon_{1/2}$ = 485 Hz).

$Ph_3PAu[SSi(SiMe_3)_3]$ (11). $HSSi(SiMe_3)_3$ (0.14 g, 0.48 mmol) dissolved in 20 mL ether was added to $Ph_3PAuN(SiMe_3)_2$ (0.30 g, 0.48 mmol) dissolved in ether (30 mL). On addition of the thiol solution, the reaction mixture remained colorless and then slowly began to take on a yellow-brown tint; a black precipitate was also noticed. The mixture was stirred for 1 h, and the solvent was removed under reduced pressure. The light brown solid was extracted with ether (40 mL), the extract was filtered, and the filtrate was concentrated to 10 mL and cooled to –40 °C for 48 h. Filtration afforded the product as pale brown, cubic crystals (0.25 g, 71%). The compound melted cleanly to an opaque orange-brown liquid from 126 to 129 °C while generating a clear condensate at the top of the melting point capillary. EI MS data show that the clear condensate generated is the asymmetric disilyl sulfide, $Me_3SiSSi(SiMe_3)_3$ (*m/z* 352 (M^+), 337 (M^+ –Me_3), 279 (M^+ – $SiMe_3$), 262, 73). IR: 1478 sh, m, 1434 s, 1253 sh, w, 1239 s, 1178 w, 1101 s, 1023 w, 995 w, 836 s, 747 s, 709 m, 688 s, 622 m, 536 s, 505 s cm^{-1}. ^1H NMR (400 MHz, C_6D_6): δ 7.40 (m, 6 H), 6.95 (m, 9 H), 0.45 (s, 27 H). $^{13}C\{^1H\}$ NMR (C_6D_6): δ 134.5, 134.3, 131.3, 129.2, 129.0, 0.63. $^{31}P\{^1H\}$ NMR (C_6D_6): δ 38.2 ($\Delta\upsilon_{1/2}$ = 105 Hz). Anal. Calcd for $C_{27}H_{42}AuPSSi_4$: C, 43.9; H, 5.73. Found: C, 43.4; H, 5.60.

X-ray Structural Studies. The accurate cell dimensions and their esd's for **1**, **3**, and **4** were derived by a least-squares fit to the setting angles of the unresolved Kα components of 24 reflections with 2θ between 22 and 24° for **1**, 22 and 25°, for **3**, and 22 and 30° for **4**. Intensity standards were measured on the diffractometer using graphite-monochromated Mo Kα radiation every 1 h of data collection. Intensity standards for **1**, **3**, and **4** over the data collection period showed 16.6, 2.1, and 1.1% losses in intensity, respectively. For each compound, three reflections were checked after every 200 measurements as orientation checks. Crystal

Table I. Crystallographic Parameters for **1**, **3**, and **4**

	1	3	4
formula	$C_{10}H_{27}AuSi_3Te$	$C_{10}H_{27}AuSSi_3$	$C_{28}H_{42}AuPSi_3Te$
mol wt	556.14	460.61	818.44
space group	$P2_12_12_1$	$P2_1/c$	$P2_1/n$
a/Å	15.295(2)	14.976(2)	9.748(3)
b/Å	16.011(2)	18.99(1)	21.472(5)
c/Å	29.971(6)	27.622(5)	15.684(3)
α/deg	90	90	90
β/deg	90	102.83(2)	100.37(2)
γ/deg	90	90	90
V/Å^3	7340(4)	7659(5)	3229(1)
Z	4	4	4
d_{calcd}/g cm^{-3}	2.013	1.598	1.683
cryst size/mm	0.25 × 0.15 × 0.18	0.20 × 0.30 × 0.40	0.30 × 0.30 × 0.10
radiation (λ/Å)	Mo Kα (0.710 73)	Mo Kα (0.710 73)	Mo Kα (0.710 73)
scan mode	ω	θ–2θ	θ–2θ
2θ range/deg	3–45	3–45	3–45
collection range	$+h,+k,+l$	$+h,+k,\pm l$	$+h,+k,\pm l$
abs coeff, μ	97.39	79.39	56.09
no. of unique reflns	5333	9966	4646
no. of reflns with $F^2 > 3\sigma(F^2)$	3232	5953	3182
final R, R_w	0.0512, 0.0446	0.0500, 0.0569	0.0485, 0.0573
T/°C	-90	-111	-111

orientation was redetermined if any of the reflections were offset by more than 0.10° from their predicted positions; reorientations for **1**, **3**, and **4** were carried out six times, two times and one time, respectively. Linear corrections for decay and appropriate absorption corrections were made for each compound.

Each crystal structure determination was solved by direct methods using the SHELXS-86 program.[29] Positional and thermal parameters were refined by the block-diagonalized-matrix least-squares method. The minimized function was $\sum w(|F_o| - |F_c|)^2$, where w is the weight of a given observation. The p factor, used to reduce the weight of intense reflections, was set to 0.02 for **1** and 0.04 for **3** and **4**. In the final cycle of the refinement, all parameter shift/error values were less than 0.01σ. The analytical forms of the scattering factor tables for the neutral atoms were used, and all scattering factors were corrected for both real and imaginary components of anomalous dispersion. The largest peaks in the final difference Fourier maps for **1**, **3**, and **4** were 1.28, 1.50, and 2.96 e/Å^3, respectively, and the lowest excursions were –0.38, –0.38, and –0.82 e/Å^3, respectively. A summary of data collection and refinement parameters is given in Table I. Positional and thermal parameters of the non-hydrogen atoms for each compound are given as supplementary material.

$Au_4[TeC(SiMe_3)_3]_4$ (1). Transparent, colorless, hexagonally *shaped* crystals were obtained by slow crystallization at ambient temperatures from warm benzene. A suitable crystal was mounted on a glass fiber using Paratone N hydrocarbon oil. The crystal was transferred to an Enraf-Nonius CAD-4 diffractometer, centered in the beam, and cooled to -90 °C. The unit cell was determined to be primitive orthorhombic with space group $P2_12_12_1$. The 5333 unique raw intensities were converted to structure factor amplitudes and their esds by correction for scan speed, background, and Lorentz and polarization effects. Hydrogen atoms were assigned idealized locations and were included in structure factor calculations, but were not refined. Some of the $SiMe_3$ groups in the molecule were disordered, and this was modeled accordingly. Due to difficulties during refinement, several Si atoms and all of the C atoms in the structure were refined with isotropic thermal parameters. The final residuals for 338 variables refined against the 3232 data for which $F^2 > 3\sigma(F^2)$ were $R = 0.0512$, $R_w = 0.0446$, and GOF = 1.271.

$Au_4[SC(SiMe_3)_3]_4$ (3). Transparent, colorless, rectangular crystals were grown from concentrated hexane at –40 °C. One fragment was mounted in air using a polycyanoacrylate cement and cooled to –111 °C. The unit cell was determined to be primitive monoclinic with space group $P2_1/c$. The 9966 unique reflections were treated as discussed above. Hydrogen atoms were assigned idealized locations and were included in structure factor calculations, but were not refined. As in the crystal structure for **1**, a single $SiMe_3$ group displayed a *clear* disordering. Si7, Si8, Si9 (72.5% occupancy), Si7′, Si8′, Si9′ (27.5% occupancy), and C3 were all refined with isotropic thermal parameters due to this disorder. One molecule of disordered hexane was discovered in association with each $Au_4[SC(SiMe_3)_3]_4$ tetramer within the unit cell. The hexane molecule (C100–C106) was modeled as five full (100%) occupancy carbon atoms and two half (50%) occupancy carbon atoms, all refined with isotropic thermal parameters. The final residuals for 561 variables refined against the 5953 data for which $F^2 > 3\sigma(F^2)$ were $R = 0.0500$, $R_w = 0.0569$, and GOF = 1.601.

$Ph_3PAu[TeC(SiMe_3)_3]$ (4). Yellow crystals suitable for X-ray diffraction were grown from concentrated diethyl ether at –40 °C. One fragment was mounted in Paratone N hydrocarbon oil and cooled to –111 °C. The unit cell was determined to be primitive monoclinic with space group $P2_1/n$. The 4646 unique reflections were treated as discussed above. Hydrogen atoms were assigned idealized locations and were included in structure factor calculations, but were not refined. The final residuals for 307 variables refined against the 3182 data for which $F^2 > 3\sigma(F^2)$ were $R = 0.0485$, $R_w = 0.0573$, and GOF = 1.704.

Results and Discussion

Gold(I) Alkanechalcogenolates. Metatheses between AuCl(THT) and lithium alkanechalcogenolates in benzene lead to a series of novel, homoleptic gold(I) compounds (eq 1). Crystallization of these derivatives from concentrated benzene at room temperature, or from hexane at lower temperatures, provides the materials in isolated yields ranging from 42 to 69%. The colorless compounds are all stable to air and water. As expected, they are easily converted to their respective triphenylphosphine adducts, **4**–**6**, by addition of stoichiometric amounts of the Lewis base to solutions of the homoleptic compounds. This is most notable in the transformation of **1** to **4**, where addition of 1 equiv of PPh_3 to colorless benzene-d_6 solutions of **1** leads to an immediate color change to yellow. When 2 or 3 mol equiv of PPh_3 is added, $^{31}P\{^1H\}$ NMR data suggest that fast exchange of PPh_3 occurs, as an averaged chemical shift, offset toward free PPh_3 (–4.8 ppm), is observed.

$$\mathrm{AuCl(THT)} + \mathrm{LiER} \xrightarrow[-\mathrm{THT}]{-\mathrm{LiCl}} \mathrm{Au(ER)} \qquad (1)$$

$$\begin{aligned} &\mathbf{1}, \mathrm{E} = \mathrm{Te} \\ &\mathbf{2}, \mathrm{E} = \mathrm{Se} \\ &\mathbf{3}, \mathrm{E} = \mathrm{S} \end{aligned}$$

$$\mathrm{R} = \mathrm{C(SiMe_3)_3}$$

These compounds were also prepared by reaction of Ph_3PAuCl and the lithium chalcogenolates in diethyl ether, or by protonolysis of the gold(I) bis(trimethylsilyl)amide $Ph_3PAuN(SiMe_3)_2$ with the chalcogenol in hexane (eqs 2 and 3). Both pathways lead to the chalcogenolates in nearly identical yields (*ca.* 75%). Like their homoleptic counterparts, these derivatives are again stable

---

[29] Sheldrick, G. M. *Crystallographic Computing 3*; Oxford University Press: Oxford, U.K., 1985; p 175.

$$Ph_3PAuCl + LiER \rightarrow Ph_3PAu(ER) + LiCl \quad (2)$$

$$Ph_3PAuN(SiMe_3)_2 + HER \rightarrow Ph_3PAu(ER) + HN(SiMe_3)_2 \quad (3)$$

to air and water. In common with most gold(I) complexes, these adducts are colorless; the tellurolate **4**, however, is yellow.[10]

The $^{31}P\{^1H\}$ NMR data for the triphenylphosphine adducts are all very similar, with chemical shifts ranging from 37 to 40 ppm, in accord with related (triphenylphosphine)gold(I) thiolates[15] and selenolates.[10,11,13,14] Unfortunately, these signals are quite broad and, in the case of the tellurolate and selenolate derivatives, contain no coupling information from ^{125}Te or ^{77}Se. For **4**, variable-temperature NMR experiments from −90 to +60 °C still failed to resolve any $^2J_{PTe}$ coupling. Similarly, in the $^{125}Te\{^1H\}$ variable-temperature NMR spectra of **4**, no $^2J_{TeP}$ was detected.

Gold(I) Silane- and Germanechalcogenolates. As with the alkyl derivatives described above, gold(I) silane- and germanechalcogenolates are straightforwardly prepared by metathesis or protonolysis reactions. Unlike the alkyl compounds, however, **7–10** are unstable in *solution* and must be prepared at low temperatures (−78 °C). Even at −40 °C in solution, decomposition over several days prevents the crystallization and purification of these materials. In the *solid state*, both the homoleptic and triphenylphosphine derivatives are stable in air and water over the course of 1–3 h, as determined by ^{1}H NMR spectroscopy. Though **7–10** may be used as crude solids directly after isolation, LiCl may be removed by filtration of cold solutions through Celite on a Schlenk frit, followed by immediate removal of solvent.

At room temperature in solution, the homoleptic compound **7** decomposes to $Me_3SiTeSi(SiMe_3)_3$,[19] (the predominant product), $Me_3SiTeSiMe_3$,[30,31] and $(Me_3Si)_3SiTeSi(SiMe_3)_3$,[32] as shown by ^{1}H NMR spectroscopy. The triphenylphosphine analogue **9** decomposes similarly but without formation of even traces of $(Me_3Si)_3SiTeSi(SiMe_3)_3$. The only product identified when the germyl derivatives **8** and **10** decomposed in solution was the germyl telluride $Me_3SiTeGe(SiMe_3)_3$ (verified by the reaction of $(THF)_2LiTeGe(SiMe_3)_3$ with Me_3SiCl in benzene-d_6). The silanethiolate, **11**, is much more stable than **7–10**; nonetheless, after 24 h in solution, even this complex shows traces of decomposition to $Me_3SiSSi(SiMe_3)_3$.

The complex decomposition reactions for the silane- and germanetellurolates contrast with that observed for the gold(I) *alkyl* derivative which decomposes on heating to form solely $(Me_3Si)_3CTeC(SiMe_3)_3$ and, presumably, the metal telluride. Indeed, reactions of this general type, wherein chalcogenolates decompose to form metal chalcogenides and diorgano chalcogenides, now appear to be almost ubiquitous in the thermal decomposition of tellurolates and selenolates.[33-36] The gold(I) silane- and germanetellurolates are notable, therefore, as they represent the first class of compounds that fail to decompose cleanly to metal telluride and TeR_2.

^{125}Te NMR shifts for the homoleptic derivatives **7** and **8** show the expected trend relative to the alkyl analogue **1**. Thus, while the chemical shift of **1** is at −302 ppm, **7** and **8** resonate at much higher field shifts of −1112 and −1093 ppm, respectively. This trend in going from alkyl to silyl to germyl derivatives has been reported for both the corresponding lithium derivatives[22] and the tellurols[22] and qualitatively suggests a much larger and similar electronic shielding of the Te nucleus in the silyl and germyl derivatives. In common with those of the alkyl derivatives, ^{31}P NMR data for **9** and **10** were exceedingly broad with no observed couplings to ^{125}Te.

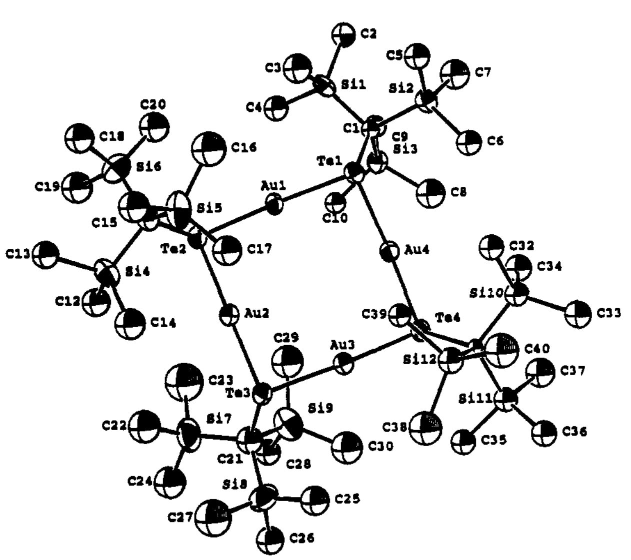

Figure 1. ORTEP view of $Au_4[TeC(SiMe_3)_3]_4$ (**1**). Hydrogens are omitted for clarity, and thermal ellipsoids are drawn at the 50% probability level.

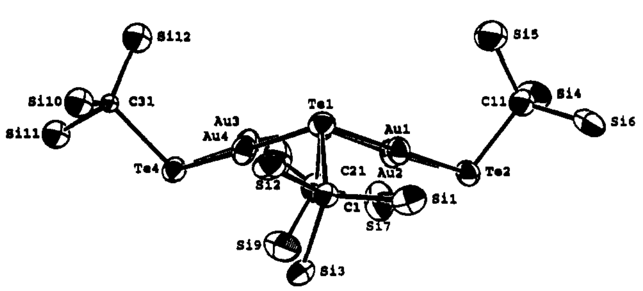

Figure 2. ORTEP view of $Au_4[TeC(SiMe_3)_3]_4$ (**1**) depicting the bent Au_4Te_4 core. Methyl groups are omitted for clarity, and thermal ellipsoids are drawn at the 50% probability level.

Table II. Selected Bond Distances (Å) and Angles (deg) for **1**

Au1–Te1	2.566(3)	Au1–Te2	2.568(3)
Au2–Te2	2.560(3)	Au2–Te3	2.564(3)
Au3–Te3	2.559(3)	Au3–Te4	2.566(3)
Au4–Te1	2.568(3)	Au4–Te4	2.567(3)
Te1–C1	2.18(3)	Te2–C11	2.19(4)
Te3–C21	2.23(4)	Te4–C31	2.26(3)
Si1–C1	1.91(3)	Si1–C2	1.86(4)
Si1–C3	1.90(5)	Si1–C4	1.86(4)
Te1–Au1–Te2	177.6(1)	Te2–Au2–Te3	175.7(1)
Te3–Au3–Te4	173.5(1)	Te1–Au4–Te4	176.8(1)
Au1–Te1–Au4	90.6(9)	Au1–Te1–C1	105.7(8)
Au4–Te1–C1	109.1(9)	Au1–Te2–Au2	87.52(8)
Au1–Te2–C11	105.5(9)	Au2–Te2–C11	105.2(9)
Au2–Te3–Au3	90.65(9)	Au2–Te3–C21	109(1)
Au3–Te3–C21	107(1)	Au3–Te4–Au4	88.32(9)
Au3–Te4–C31	109.2(8)	Au4–Te4–C31	106.7(7)
C1–Si1–C2	112(1)	C1–Si1–C3	112(1)
C1–Si1–C4	113(1)		

X-ray Crystallography. The molecular structure of **1** is shown as an ORTEP view in Figure 1, with pertinent bond lengths and angles given in Table II. Compound **1** crystallizes in the space group $P2_12_12_1$, and the screw axes are clearly evident in molecular packing diagrams. The Au_4Te_4 core is butterflied (see Figure 2), with both wings of the butterfly being nearly coplanar. One wing, comprising Te1, Au1, Te2, Te4, and Au4, is coplanar to within 0.04 Å, while the second half, Te3, Au2, Te2, Au3, and Te4, is coplanar to within 0.09 Å. The dihedral angle between

---

(30) Du Mont, W.-W.; Kroth, H. J. *Z. Naturforsch.* **1981**, *36B*, 332.
(31) Detty, M. R.; Seidler, M. D. *J. Org. Chem.* **1982**, *47*, 1354.
(32) Christou, V.; Arnold, J. *J. Am. Chem. Soc.* **1992**, *114*, 6240.
(33) Arnold, J.; Walker, J. M.; Yu, K. M.; Bonasia, P. J.; Seligson, A. L.; Bourret, E. D. *J. Cryst. Growth* **1992**, *124*, 647.
(34) Seligson, A. L.; Bonasia, P. J.; Arnold, J.; Yu, K. M.; Walker, J. M.; Bourret, E. D. *Mater. Res. Soc. Symp. Proc.* **1993**, *282*, 665.
(35) Steigerwald, M. L.; Sprinkle, C. R. *J. Am. Chem. Soc.* **1987**, *109*, 7200.
(36) Cary, D. R.; Arnold, J. *J. Am. Chem. Soc.* **1993**, *115*, 2520.
(37) Müller, A.; Dornfield, H.; Henkel, G.; Krebs, B.; Viegers, M. P. A. *Angew. Chem., Int. Ed. Engl.* **1978**, *17*, 52.

Table III. Selected Bond Distances (Å) and Angles (deg) for 3

Au1–S1	2.297(5)	Au1–S4	2.303(5)
Au2–S1	2.310(5)	Au2–S2	2.315(5)
Au3–S2	2.309(5)	Au3–S3	2.305(5)
Au4–S3	2.298(5)	Au4–S4	2.302(5)
S1–C1	1.86(2)	S2–C2	1.86(2)
S3–C3	1.88(2)	S4–C4	1.89(2)
Si1–C1	1.92(2)	Si1–C5	1.90(2)
Si1–C6	1.89(2)	Si1–C7	1.89(2)
S1–Au1–S4	177.0(2)	S1–Au2–S2	177.1(2)
S2–Au3–S3	177.5(2)	S3–Au4–S4	178.5(2)
Au1–S1–Au2	92.6(2)	Au1–S1–C1	114.9(6)
Au2–S1–C1	115.9(6)	Au2–S2–Au3	91.4(2)
Au2–S2–C2	113.7(7)	Au3–S2–C2	114.9(7)
Au3–S3–Au4	91.6(2)	Au3–S3–C3	110.8(6)
Au4–S3–C3	111.7(6)	Au1–S4–Au4	91.9(2)
Au1–S4–C4	112.4(6)	Au4–S4–C4	112.9(6)
C1–Si1–C5	112.3(9)	C1–Si1–C6	111.4(9)
C1–Si1–C7	112.3(9)		

these two least-squares planes is 144.98(6)°. Au1, Au2, Au3, and Au4 are coplanar to within 0.06 Å. All eight Au–Te bonds are remarkably similar with the average distance being 2.56(3) Å. The Te–Au–Te bonds approach linearity with an average angle of 175°, while the Au–Te–Au angles vary between 87 and 90°. Adjacent gold atoms (*e.g.* Au1, Au2 or Au3, Au4) are approximately 3.6 Å apart (the Au–Au distance in gold metal is 2.88 Å[17]); gold atoms across from one another in the tetrameric units are separated by nearly 5 Å. The $C(SiMe_3)_3$ ligands around the tetramer alternate pointing up and down in direction due most likely to the steric effects incurred on these adjacent groups, which, as mentioned above, are in close proximity. Average Te–C bonds (2.2 Å) are quite similar to the Te–C bond of 2.24(1) Å in $Ph_3PAu[TeC(SiMe_3)_3]$ discussed below. The structure of **1** may be compared to those of several structurally characterized gold tellurides, among which are the anions $[K_2Au_4Te_4(en)_4]^{2-}$ [17] and $[K_2Au_4Te_4(dmf)_2(CH_3OH)_2]^{2-}$.[17] In these anionic tellurides, the $[Au_4Te_4]^{4-}$ cores are rhombohedrally distorted planes, with average Au–Te bond lengths of 2.58 and 2.57 Å, respectively. These anions also display adjacent Au–Au contacts of 3.26 and 3.05 Å, respectively, and again, though slightly shorter, agree quite well with similar distances in **1**. In $(PPN)_2Au_2Te_4$,[18] the average Au–Te bond length is 2.55 Å.

The molecular structure of **3** is shown as an ORTEP view in Figure 3. In essence, the structure of **3** is nearly identical to that of its tellurium analogue, **1**, with the most notable deviation being the planarity of the Au_4S_4 core (see Figure 4). One half of this eight-membered ring, S1, Au1, Au2, S2, and S4, is planar to within 0.02 Å. The least-squares plane determined for S3, Au3, Au4, S2, and S4 deviates by only 0.03 Å, and the dihedral angle between these two planes is 4.2 (6)°. The four gold atoms alone are planar to within 0.006 Å; from *this* least-squares plane, S1, S2, S3, and S4 deviate by 0.121(5), –0.077(5), 0.002(5), and –0.040(5) Å, respectively. Inspection of the angles about each sulfur atom in the structure suggests a tendency toward a trigonal planar geometry and thus the planar Au_4S_4 unit; while a tendency toward pyramidalization in the structure of **1** forces the pronounced bend in the Au_4Te_4 core. The Au–S bond distances range from 2.297(5) to 2.315(5) Å, with an average bond length of 2.305(5) Å. As in the tellurium analogue, the angles around gold are virtually linear, while those about sulfur in the ring are between 91 and 92°. Adjacent gold atoms are 3.3 Å apart, while gold atoms across the ring from one another are separated by nearly 4.7 Å. These Au–Au contacts are approximately 0.3 Å shorter than similar distances in **1**, simply reflecting the smaller ring size due to sulfur atoms replacing the larger tellurium atoms. Average S–C bond lengths are 1.87(2) Å. Strähle has prepared several gold(I) thiolate derivatives, the most relevant of which is the hexameric $[(2,4,6\text{-}{}^iPr_3C_6H_2S)Au]_6$,[16] which forms a centrosymmetrical twelve-membered Au–S ring. The gold atoms are linearly coordinated with average S–Au–S angles of 176.3(1)°, and Au–S distances range from 2.278(3) to 2.295(3) Å. Adjacent gold atoms are quite distant from one another with average Au–Au contacts being 3.5642 (7) Å. In $[(2,4,6\text{-}{}^iPr_3C_6H_2S)_2Au]^-NH_4^+$,[16] the S1–Au–S2 angle is 175.6(1)° and both Au–S bonds are identical at 2.288(4) Å. In the distorted cubane-like thioaurate $[Ph_4As]_4[Au_{12}S_8]$, also prepared by Strähle,[8] metrical parameters of the planar Au_4S_4 units (Au–S = 2.237(5)–2.346(5) Å; Au–Au = 3.179(1)–3.351(1) Å, S–Au–S = 177.8(2)–179.4(2)°, Au–S–Au = 86.7(2)–93.1(2)°) are very similar to those determined for **3**. Further notable comparisons can be found in the structural characterizations of: $[Au_2(WS_4)_2]^{-2}$,[37] $[n\text{-}Bu_4N]_2[Au(S_2C_2(CN)_2^{-2})]_2$,[38] $Au_4(CH_3CS_2)_4$,[39] $[Au_2(PPh_3)_2(\mu\text{-}SCH_2Ph)](NO_3)$,[12] and $(\mu_3\text{-}S)(PPh_3Au)_3PF_6$.[9]

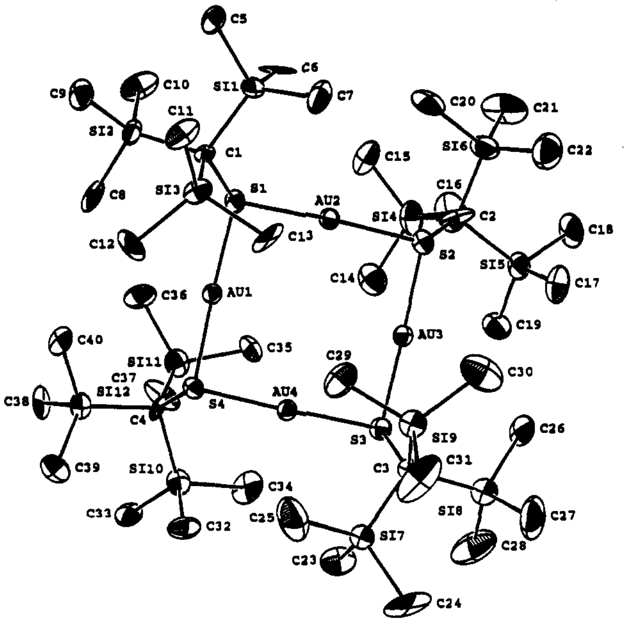

Figure 3. ORTEP view of $Au_4[SC(SiMe_3)_3]_4$ (3). Hydrogens are omitted for clarity, and thermal ellipsoids are drawn at the 50% probability level.

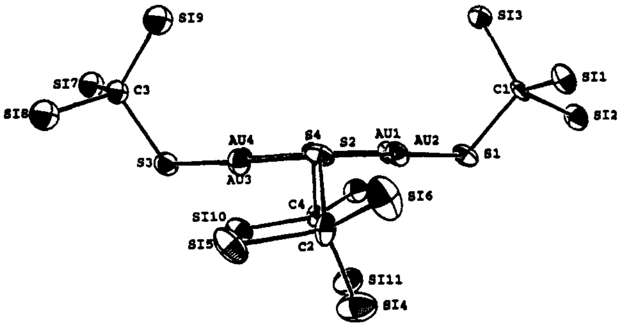

Figure 4. ORTEP view of $Au_4[SC(SiMe_3)_3]_4$ (3) depicting the planar Au_4S_4 core. Methyl groups are omitted for clarity, and thermal ellipsoids are drawn at the 50% probability level.

Figure 5 shows an ORTEP view of $Ph_3PAu[TeC(SiMe_3)_3]$ (**4**). The molecular structure shows a nearly linear Te–Au–P angle of 174.35(9)°, as expected for Au(I) complexes, and the Au–Te–C19 angle of 104.1(4)° appears to be the result of packing effects of the sterically encumbering $C(SiMe_3)_3$ groups. Furthermore, as can be seen in Figure 5, where two of the four symmetry-related molecules in the unit cell are shown, two intermolecular, van der Waals contacts of 3.740(1) Å (represented by dotted lines) are observed between Au and Te atoms (van der Waals radii of Au and Te are 1.66 and 2.06 Å, respectively[40]).

---

(38) Khan, M. N. I.; Fackler, J. P., Jr.; King, C.; Wang, J. C.; Wang, S. *Inorg. Chem.* **1988**, *27*, 1672.

(39) Chiari, B.; Piovesana, O.; Tarantelli, T.; Zanazzi, P. F. *Inorg. Chem.* **1985**, *24*, 366.

(40) Bondi, A. *J. Phys. Chem.* **1964**, *68*, 441.

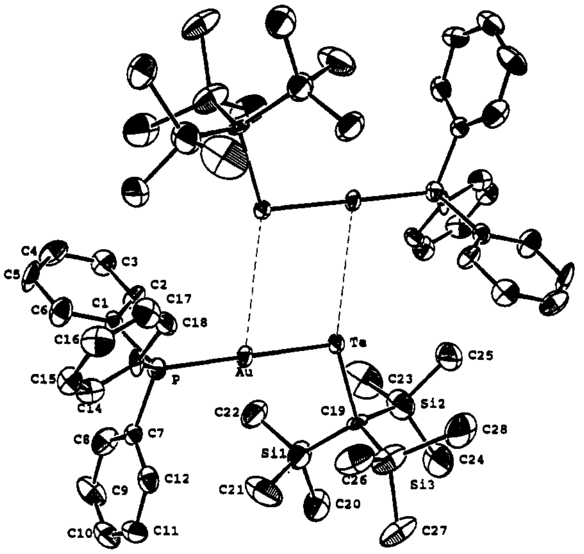

Figure 5. ORTEP view of $Ph_3PAuTeC(SiMe_3)_3$ (**4**) depicting two molecules in van der Waals contact. Hydrogens are omitted for clarity, and thermal ellipsoids are drawn at the 50% probability level.

Table IV. Selected Bond Distances (Å) and Angles (deg) for **4**

Au–Te	2.566(1)	Au–P	2.286(4)
Te–C19	2.23(1)	P–C1	1.81(1)
P–C7	1.82(1)	P–C13	1.80(1)
Te–Au–P	174.35(9)	Au–Te–C19	104.1(4)
Au–P–C1	111.5(5)	Au–P–C7	111.7(4)
Au–P–C13	118.1(4)	Te–C19–Si1	110.9(6)
Te–C19–Si2	101.8(6)	Te–C19–Si3	105.8(6)

The intramolecular Au–Te distance of 2.566(1) Å is nearly identical to the average Au–Te distance observed in the homoleptic derivative. While a number of (triphenylphosphine)gold(I) thiolates and selenolates have been prepared (see references above), we are unaware of any reports of tellurolates. Du Mont has prepared $Ph_3PAu[Se(2,4,6\text{-}^tBu_3C_6H_2)]$,[11] but there has been no report of the compound's solid-state structure. Similarly, Delgado has prepared a variety of non structurally characterized $Ph_3PAu[SR]$ complexes where R = C_2H_5, C_6H_5, $CH_2C_6H_5$, C_6F_5, 2,4,6-$Me_3C_6H_2$, ^{i}Pr, and ^{t}Bu.[15] Jones has structurally characterized $Ph_3PAu[SePh]$ and $[(Ph_3PAu)_2SePh]^+SbF_6^-$ [10]. In the former compound, the Se–Au–P angle is nearly linear (176–180°), and the Au–Se–*ipso*-C angle is approximately 105.5(2)°. $Ph_3PAu[SePh]$ crystallizes with two independent molecules in the asymmetric unit, and the authors propose that a Au–Au contact of 3.118 (1) Å may suggest aggregation into a loose dimer. Although we observe no such Au–Au contact in the structure of **4**, this phenomenon of gold aggregation in molecules is rather commonplace when allowed by steric conditions.[41–43] In **4**, the closest heavy-atom contacts between molecules are Au–Au (4.995 (1) Å), Te–Te (4.025(2) Å), and Au–Te (3.740(1) Å).

Acknowledgment. Financial support from the National Science Foundation (Grant CHE-92-10406) is gratefully acknowledged.

Supplementary Material Available: Tables of temperature factor expressions, positional parameters, and intramolecular distances and angles for **1**, **3**, and **4** and tables of least-squares planes for **3** and **4** (35 pages). Ordering information is given on any current masthead page.

---

(41) Schmidbaur, H.; Weidenhiller, G.; Steigelmann, O.; Müller, G. *Z. Naturforsch.* **1990**, *45B*, 747.
(42) Schmidbaur, H.; Weidenhiller, G.; Steigelmann, O.; Müller, G. *Chem. Ber.* **1990**, *123*, 285.
(43) Nakamoto, M.; Hiller, W.; Schmidbaur, H. *Chem. Ber.* **1993**, *126*, 605.